J Neurophysiol 103: 3398–3406, 2010.
First published April 21, 2010; doi:10.1152/jn.00141.2010.

Functional Networks in the Anesthetized Rat Brain Revealed by Independent Component Analysis of Resting-State fMRI

R. Matthew Hutchison,[1,2,7] Seyed M. Mirsattari,[1,3–7] Craig K. Jones,[7] Joseph S. Gati,[7] and L. Stan Leung[1,2]
[1]*Graduate Program in Neuroscience,* [2]*Departments of Physiology and Pharmacology,* [3]*Clinical Neurological Sciences,* [4]*Medical Biophysics,* [5]*Medical Imaging, and* [6]*Psychology, University of Western Ontario, London; and* [7]*Robarts Research Institute, London, Ontario, Canada*

Submitted 2 February 2010; accepted in final form 19 April 2010

Hutchison RM, Mirsattari SM, Jones CK, Gati JS, Leung LS. Functional networks in the anesthetized rat brain revealed by independent component analysis of resting-state fMRI. *J Neurophysiol* 103: 3398–3406, 2010. First published April 21, 2010; doi:10.1152/jn.00141.2010. The rodent brain is organized into functional networks that can be studied through examination of synchronized low-frequency spontaneous fluctuations (LFFs) of the functional magnetic resonance imaging -blood-oxygen-level-dependent (BOLD) signal. In this study, resting networks of LFFs were estimated from the whole-brain BOLD signals using independent component analysis (ICA). ICA provides a hypothesis-free technique for determining the functional connectivity map that does not require a priori selection of a seed region. Twenty Long-Evans rats were anesthetized with isoflurane (1%, $n = 10$) or ketamine/xylazine (50/6 mg $\cdot$ kg^{-1} $\cdot$ h^{-1} ip, $n = 10$) and imaged for 5–10 min in a 9.4 T MR scanner without experimental stimulation or task requirement. Independent, synchronous LFFs of BOLD signals were found to exist in clustered, bilaterally symmetric regions of both cortical and subcortical structures, including primary and secondary somatosensory cortices, motor cortices, visual cortices, posterior and anterior cingulate cortices, hippocampi, caudate-putamen, and thalamic and hypothalamic nuclei. The somatosensory and motor cortices typically demonstrated both symmetric and asymmetric components with unique frequency profiles. Similar independent network components were found under isoflurane and ketamine/xylazine anesthesia. The report demonstrates, for the first time, 12 independent resting networks that are bilaterally synchronous in different cortical and subcortical areas of the rat brain.

INTRODUCTION

Resting-state functional magnetic resonance imaging (fMRI) examines temporal correlations in the blood-oxygen-level-dependent (BOLD) signal in the absence of a specific task. It is believed that the coherence in low-frequency baseline fluctuations (LFFs; 0.01–0.1 Hz) arises from neurovascular mechanisms regulating blood flow and is presumed to reflect intrinsic functional connectivity of the brain (Biswal et al. 1995). The widely separated brain regions identified with resting-state analysis have also been shown to reveal structural connectivity (Greicius et al. 2009). Distinct networks serving vision, motor, auditory, language, cognitive, and default-mode functions (Beckmann et al. 2005; Hampson et al. 2002; Raichle et al. 2001) have been identified in humans. The networks manifest highly organized patterns of coherence across mammalian species (Pawela et al. 2008; Vincent et al. 2006, 2007) and persist regardless of the depth or type of general anesthetic (Kannurpatti et al. 2008; Lu et al. 2007; Vincent et al. 2007; Zhao et al. 2008).

Address for reprint requests and other correspondence: L. Stan Leung, Dept. Physiology and Pharmacology, University of Western Ontario, Medical Sciences Bldg. Rm. 236, London, Ontario, N6A 5C1 Canada (E-mail: sleung@uwo.ca).

Although the precise physiological origin and mechanism of regulation of LFFs have not been fully explained, studies have demonstrated changes in functional networks in a variety of human disease states including Alzheimer's disease (Greicius et al. 2004), autism (Cherkassky et al. 2006), depression (Greicius et al. 2007), epilepsy (Waites et al. 2006), multiple sclerosis (Lowe et al. 2002), and schizophrenia (Bluhm et al. 2007). As disruptions in functional connectivity have been suggested as possible causes or consequences of pathological states, there is increased interest to extend the study of resting-state networks to animal models. Genetic, physical, and chemical models exist for a variety of disease states and afford experimental manipulations not possible in humans. Through this avenue, we will gain a better understanding of the physiological mechanisms of entrainment, regulation, and fluctuation of the synchronous hemodynamic signals.

Initial examinations of physiological fluctuations in BOLD signals of rats have revealed substantial inter-hemispheric synchrony across multiple brain areas with reproducible, independent, homologous networks observed for the primary somatosensory cortex, primary visual cortex, and caudate-putamen (Kannurpatti et al. 2008; Lu et al. 2007; Pawela et al. 2008, 2010; Zhao et al. 2008). This is in accordance with network connectivity patterns seen in human (Cordes et al. 2001) and monkey (Vincent et al. 2007) studies that demonstrated bilateral motor, auditory, and visual networks. In humans, these networks have been shown to be present at birth (Fransson et al. 2009; Lin et al. 2008). Higher order resting-state networks also exhibit high degrees of synchronization between cortical and subcortical inter-hemispheric homologues (Beckmann et al. 2005).

Spatial functional connectivity maps of the rat are typically inferred by a cross-correlation analysis of the voxel-wise fMRI recordings against a reference time course. The seed voxel or region is typically chosen from an area found to be active during a stimulation paradigm and believed to be of functional relevance (Beckmann et al. 2005). The technique fundamentally tests a specific hypothesis and the functional connectivity map greatly depends on the choice of the seed region and on the correlational value used to threshold each map (Cole et al. 2010). Difficulties with the technique are also apparent when attempting to design a stimulation task to elicit robust and localized hemodynamic changes in specialized brain areas. The matter is further complicated by the use of anesthesia, typical of most fMRI experiments with rodents, which may prevent the necessary motor, visual, or auditory responses. It is for these reasons that most investigations have primarily focused

on the connectivity of the somatosensory cortices because the latter could be easily identified by the BOLD signal increase following electrical paw stimulation in the rat (Zhao et al. 2008).

To avoid the constraints of these analytical techniques in the estimation of LFFs, hypothesis-independent, exploratory techniques such as ICA have been applied to functional data sets (Beckmann et al. 2005; Correa et al. 2007; Greicius et al. 2004). ICA is a statistical technique that uses a linear model to decompose independent, uncorrelated, and non-Gaussian datasets into distinct subparts (Vigário et al. 2000). In terms of examining the BOLD signal, ICA is able to identify signal fluctuations by virtue of their spatial and temporal profiles without the need to specify an explicit model or voxel. The nonoverlapping, temporally coherent functional networks are extracted without constraining the temporal domain and are a priori independent (McKeown et al. 1998). In the present study, we used ICA to examine the spatiotemporal characteristics of the LFFs of anesthetized rats at rest with two different anesthetic regimes. Similar to network patterns observed in monkeys and humans, it is hypothesized that multiple independent, bilaterally synchronous resting-state networks exist in cortical and subcortical areas of the rat brain.

METHODS

Animal usage and preparation

A total of 20 male Long-Evans rats (250–350 g body weight) were used. Animals were provided with normal food and water ad libitum and subjected to a 12:12 h light/dark cycle. All experiments were carried out in accordance with the guidelines established by the Canadian Council on Animal Care and approved by the Animal Use Committee of the University of Western Ontario.

In isoflurane animals ($n = 10$), general anesthesia was induced with 5% isoflurane mixed with oxygen, using a calibrated vaporizer (Harvard Apparatus, Holliston, MA). Isoflurane was then maintained at 2% while the animal was being prepared in the stereotaxic frame and then lowered to 1% following insertion into the magnet for image acquisition. At least 30 min was allowed for the isoflurane level and global hemodynamics to stabilize at the 1% concentration, during which shimming and image localization were performed. The gaseous mixture was delivered to a nosecone for spontaneous respiration throughout the experiment. Ketamine/xylazine animals ($n = 10$) were initially anesthetized with a dose of 80 mg/kg ip ketamine and 10 mg/kg ip xylazine and then maintained with a continuous infusion of ketamine ($50\ mg \cdot kg^{-1} \cdot h^{-1}$ ip) xylazine ($6\ mg \cdot kg^{-1} \cdot h^{-1}$ ip), and saline ($0.8\ ml \cdot kg^{-1} \cdot h^{-1}$ ip) using a syringe pump (PHD2000, Harvard Apparatus, Holliston, MA). Once anesthetized, the rats were secured in a custom-built nylon stereotaxic frame (Mirsattari et al. 2005) using ear and bite bars to prevent head motion. The rectal temperature was measured with a fiber-optic probe and maintained at ~37°C via a feedback-controlled warm air system (MR compatible small animal monitoring and gating system, SA Instruments, Stoney Brook, NY) along with a heated feedback-controlled, water-circulated heating pad (TP500, Gaymar Industries, Orchard Park, NY). Respiration was monitored using a pneumatic pillow (SA Instruments) taped to the chest wall of the rat. Heart rate and blood oxygen saturation were measured using an MR compatible pulse oximeter (8600V, Nonin Medical, Plymouth, MN) positioned on the hindpaw. Physiological parameters were in the normal range (temperature: 36.5–37°C, heart rate: 250–370 beat/min, breathing: 60–90 breath/min, oxygen saturation: >95%) throughout the duration of the experiment.

MRI acquisition

All experiments were performed using a Varian DirectDrive imaging console (Palo Alto, CA) with a Magnex 31 cm actively shielded 9.4 T horizontal bore magnet equipped with an actively shielded gradient set (12 cm ID, SR = $3{,}000\ mT \cdot m^{-1} \cdot s^{-1}$; Yarnton, UK). An optimized home-built 1.5 × 2.0 cm linear transmit-receive surface coil was positioned proximally to the anterior aspect of the rat's head for imaging. An automated shimming algorithm was used to optimize the magnetic field over our imaging volume of interest using RASTAMAP (Klassen and Menon 2004). Ten or 13 1-mm-thick coronal or horizontal slices covering the brain were selected. A fast spin echo (FSE) anatomical (effective echo train (TE) = 40 ms, reception time (TR) = 5 s, echo train length (ETL) = 4) was acquired with a 256 × 256 matrix and a field of view (FOV) of 25.6 × 25.6 mm. Functional images were acquired using an echo planar imaging sequence (TE = 15 ms, volume acquisition (Vol Acq) time = 1,000 ms, flip angle = 40°), with a 64 × 64 matrix, and a FOV of 25.6 × 25.6 mm, corresponding to an in-plane spatial resolution of 400 × 400 μm^2. For each fMRI run, 300 (1 isoflurane anesthetized rat, 3 ketamine/xylazine anesthetized rats) or 600 (9 isoflurane anesthetized rats, 7 ketamine/xylazine anesthetized rats) images were acquired over 5 or 10 min, respectively, while the rat was resting in the scanner.

Image analysis

Preprocessing steps were carried out in BrainVoyager QX (www.BrainVoyager.com). Trilinear three-dimensional (3D) motion correction and spatial smoothing using a Gaussian filter (full-width at half-maximum = 1.2 mm) was applied to each data set. An eighth-order Butterworth low-pass filter with a cutoff at 0.1 Hz was implemented in MATLAB (Mathworks, Natick, MA) and applied to all voxel time courses on a voxel by voxel basis covering the entire brain (Hampson et al. 2002). Following data reduction using principal component analysis (PCA) in which >99.5% of the variability in the data were retained, the images were subjected to spatial independent component analysis (ICA) using the infomax algorithm (Bell and Sejnowski 1995) implemented in the GIFT software package (GIFT 2008). Currently, there are no established criteria to guide the selection of an optimal number of components for a given data set. Using a similar strategy employed by Calhoun et al. (2001), 40 components were chosen for each rat as this preserves most of the variance in the data and gives a manageable number of components. The independent components were then scaled to empirically derived z-scores by dividing by the SD of the original time sequence. The z-scores approximate the temporal correlation between each voxel and the associated component where the magnitude of the z-score specifies the strength of the linear relationship (Mannell et al. 2009). A z-score value of 1 was used as the lower limit threshold of functional connectivity. The ICA derived components of each rat were then visually inspected and labeled based on the spatial patterns in reference to known anatomical and functional locations (Paxinos and Watson 1986). Components were not regressed against a previously defined template, a common technique performed in human ICA investigations (Greicius et al. 2004). There are currently no standardized rat templates available and the creation of the template would require the acquisition of a separate dataset that would then have to be manually labeled, negating the benefit of the template.

Functional connectivity was also examined using seed-region analysis in four rats (2 from each anesthetic group) to demonstrate that ICA results corroborated traditional analysis strategies. Data were preprocessed in the same manner used for ICA. Spherical seed regions (0.5 mm radius) were selected in the right medial frontal cortex, parietal cortex, hippocampus, caudate-putamen, thalamus, and hypothalamus using a rat atlas (Paxinos and Watson 1986) without the use of a functional localizer as no functional paradigms were performed. The extracted BOLD time course of each seed region was averaged and then cross-correlated with all voxels within the brain to derive a

corresponding connectivity map, displayed using different thresholds. The analysis was implemented using the resting-state fMRI data analysis toolkit (Rest 2007).

RESULTS

Without a priori defined templates or constrained modeling, clearly identifiable regions were apparent from visual inspection alone. ICA was able to extract bilateral synchronous activity of multiple brain structures in all 20 rats of which 10 rats anesthetized with isoflurane and the remaining 10 rats with ketamine/xylazine (METHODS). The neocortex was separated into eight components corresponding to functional brain areas. These were the medial and lateral frontal cortex (primary and secondary motor areas), parietal cortex (primary somatosensory area), temporoparietal cortex (secondary somatosensory area), medial (visual area) and lateral occipital (auditory) cortex, and the posterior and anterior cingulate cortex (Fig. 1). The most clearly identifiable subcortical areas were the caudate-putamen, hippocampus, thalamus, and hypothalamus (Fig. 1). The thalamus and hypothalamus were not separated into individual nuclei as the resolution, smoothing, and lowered signal-to-noise ratio distal to the position of the surface coil prevented accurate identification. Five rats also showed a distinctive cerebellar component; however, in 15 rats, the field of view did not encompass a large enough proportion of the cerebellum to allow objective comparison or grouping.

As presented in Table 1, the majority of rats were found to have a corresponding bilateral component for each of the identified brain areas. It was also found that some rats had one or two separate components for the analogous structure in addition to or in the place of the bilateral component (Table 2). Network connectivity was present regardless of the type of anesthetic and a χ^2 test for independence showed there was no significant difference between the two groups in terms of the number of rats demonstrating each particular anatomically relevant bilateral component [$\chi^2(11) = 2.21$, $P = 0.998$].

Frequency analysis of the BOLD time courses of components of individual rats (Fig. 2*B*) showed power at low frequencies of <0.1 Hz (*D*). Time-spectral analysis showed frequency peaks and distribution that varied over time (Fig. 2*C*). While the power spectrum (and corresponding time function) of each ICA component was distinct in each individual rat, averaging the ICA components of the same structure across rats did not reveal consistent frequency peaks. The latter may

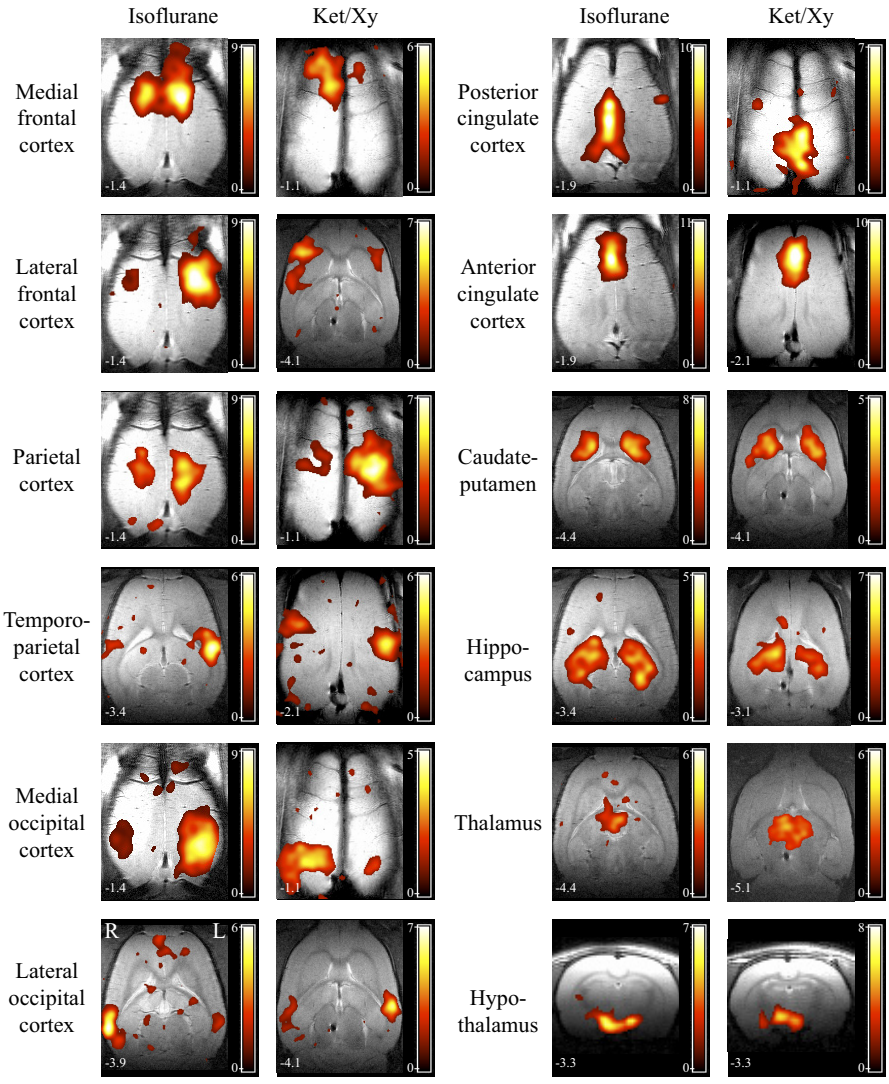

FIG. 1. Homologous resting-state networks of representative isoflurane and ketamine/xylazine (Ket/Xy) anesthetized rats derived using independent component analysis (ICA) of blood-oxygen-level-dependent (BOLD) functional time courses overlaid on the respective anatomical images (Paxinos and Watson 1986). Except for the hypothalamus, horizontal slices were obtained from 1 rat, anesthetized with isoflurane or Ket/Xy, with distance (mm) ventral to bregma shown in the left lower corner. The hypothalamus component map was derived from a different rat for each anesthetic, and is displayed in a coronal orientation referenced posterior to bregma (mm), to allow better anatomical localization.

TABLE 1. *Number of rats in isoflurane and ketamine/xylazine anesthesia groups that had independent spatial components corresponding to anatomical locations (Paxinos and Watson 1986) in both hemispheres (bilaterally synchronous), or in the left or right hemisphere*

Anatomical Brain Area (Functional Representation)	Isoflurane			Ketamine/xylazine		
	Bilateral	Left	Right	Bilateral	Left	Right
Medial frontal cortex (primary motor area)	10	3	4	10	1	3
Lateral frontal cortex (secondary motor area)	7	3	8	10	3	2
Parietal cortex (primary somatosensory area)	9	9	8	10	6	5
Temporoparietal cortex (secondary somatosensory area)	3	7	9	7	3	3
Medial occipital cortex (primary visual area)	10	8	6	10	5	4
Lateral occipital cortex (primary auditory area)	6	3	4	6	4	4
Posterior cingulate cortex	10	—	—	10	—	—
Anterior cingulate cortex	9	—	—	10	—	—
Caudate-Putamen	7	2	2	10	2	2
Hippocampus	10	4	2	10	2	2
Thalamus	8	—	—	7	—	—
Hypothalamus	5	—	—	6	—	—

A single rat may have both bila- and unilateral components corresponding to a functional area. See Table 2 for distribution of components. The posterior cingulate cortex, anterior cingulate cortex, thalamus, and hypothalamus were not grouped into left and right hemisphere components due to restrictions imposed by the resolution $n = 10$ for both isoflurane and Ketamine/xylazine.

be expected because ICA does not separate components based on the frequency of the time course.

Seed-region analysis revealed synchronized LFFs of the BOLD signal between the seed-region and analogous area in the contralateral hemisphere for both cortical and subcortical areas in all four rats examined. Functional connectivity maps of the two representative rats from each anesthetic group are shown in Fig. 3 in which a spherical seed was placed in the right medial frontal cortex (MFC; primary motor cortex; Fig. 3*A*), parietal cortex (primary somatosensory area; SSI; *B*), hippocampus (Hp; *C*), caudate-putamen (CPu; *D*), thalamus (Th; *E*), or hypothalamus (Ht; *F*). LFF synchronization was apparent under ketamine/xylazine (Fig. 3, *rats 1* and *2*) and isoflurane (Fig. 3, *rats 3* and *4*) anesthesia. The functional maps showed a variable degree of synchronization with other structures and different thresholds were needed to display the bilateral hemispheric connectivity. One rat did not have a prominent network in the caudate-putamen (Fig. 3*D, rat 4*).

DISCUSSION

Functional resting-state networks in the rodent brain have been inferred based on synchronous fluctuations of the hemodynamic signals investigated using ICA. With this technique, the entire brain was probed for functional network connectivity without requiring seed regions or the stimulus tasks necessary to activate brain areas. Spontaneous BOLD resting-state fluctuations were found to be bilaterally synchronous across multiple brain structures including the hippocampus, hypothalamus, thalamus, cingulate cortices, auditory cortices, and sensorimotor cortical areas. Such a large number of independent networks ($\leq$12 coexisting in a particular animal) have not been reported before, and in particular, specific, homologous functional networks have not been reported for the auditory cortices, secondary somatosensory and motor cortices, posterior and anterior cortices, hippocampus, thalamus and hypothalamus, as shown in a summary of the literature (Table 3). Connectivity between some of these areas has been observed in more diffuse, possibly higher-order visual and sensorimotor networks (Pawela et al. 2008) although these do not represent independent networks.

The functional connectivity revealed by ICA could also be shown using seed-region analysis. However, the size and placement of the seed within a brain structure was subjective, and the resulting functional connectivity maps were much more diffuse despite the use of variable thresholds. ICA was better able to identify bilateral networks among the noise

TABLE 2. *Distribution of rats that had uni- and bilateral components corresponding to anatomical locations*

Anatomical Brain Area	Bilateral and No Unilateral Components	Bilateral and One Unilateral Component	Bilateral and Two Unilateral Components	Two Unilateral Components	One Unilateral Component	No Component
Medial frontal cortex (primary motor area)	12 (60)	5 (25)	3 (15)	0 (0)	0 (0)	0 (0)
Lateral frontal cortex (secondary motor area)	7 (35)	7 (35)	3 (15)	1 (5)	2 (10)	0 (0)
Parietal cortex (primary somatosensory area)	1 (5)	10 (50)	8 (40)	1 (5)	0 (0)	0 (0)
Temporoparietal cortex (secondary somatosensory area)	4 (20)	4 (20)	2 (10)	3 (15)	7 (35)	0 (0)
Medial occipital cortex (primary visual area)	6 (30)	5 (25)	9 (45)	0 (0)	0 (0)	0 (0)
Lateral occipital cortex (primary auditory area)	5 (25)	6 (30)	1 (5)	4 (20)	1 (5)	3 (15)
Caudate-Putamen	13 (65)	2 (10)	2 (10)	1 (5)	1 (5)	1 (5)
Hippocampus	11 (55)	7 (35)	2 (10)	0 (0)	0 (0)	0 (0)

$n = 20$, combining 10 rats under isoflurane and 10 under Ketamine/xylazine anesthetic. Data are from Paxinos and Watson (1986). Values in parentheses are percentages.

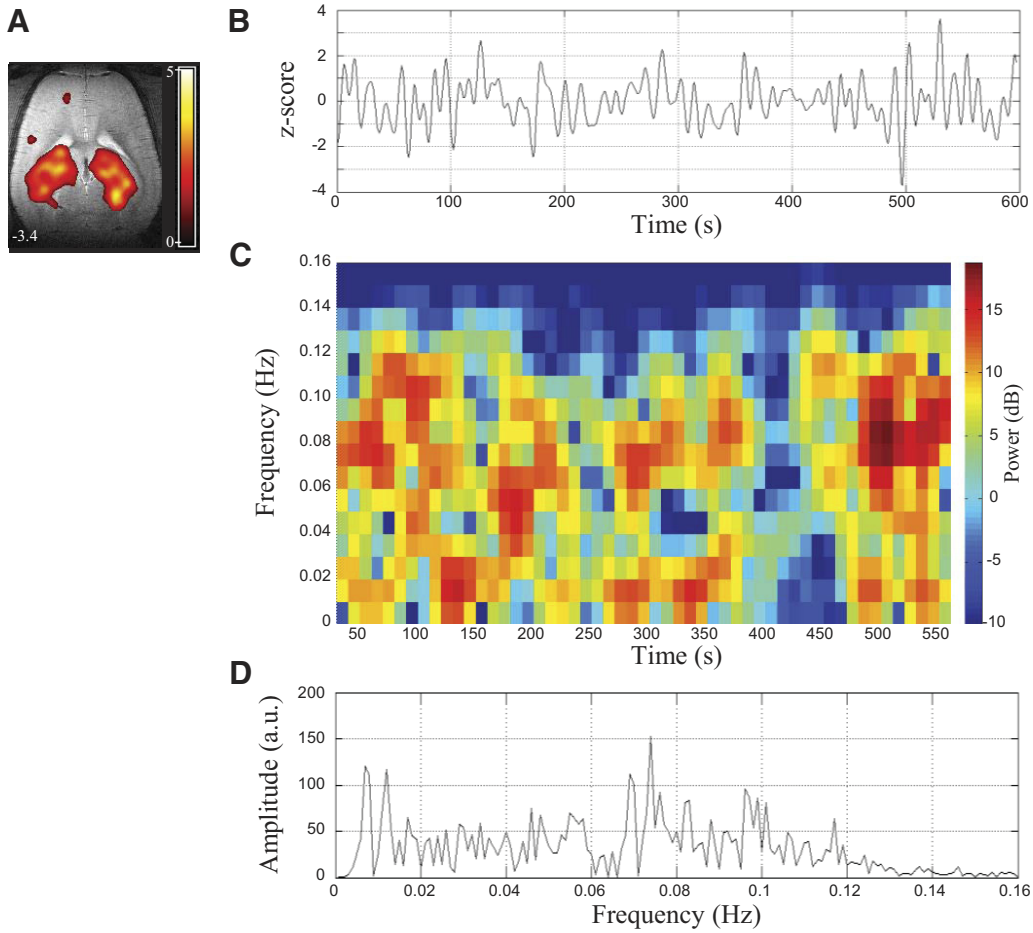

FIG. 2. Frequency analysis of the hippocampus component isolated by independent component analysis in a representative rat under isoflurane anesthesia, showing spatial connectivity map (*A*), time course (*B*), time-frequency analysis of the time course (*C*), and amplitude spectrum in arbitrary units (a.u.) of the entire time course (*D*).

without the assumption of seed regions or functional paradigms.

Connectivity patterns

The brain relies on constant inter-hemispheric communication for coherent integration of cognition and behavior (Compton 2002). It has been shown that hemispheric interaction is critical for a unified representation of world (Houzel et al. 2002), coordinating movement (Gerloff and Andres 2002), attentional processing (Banich 1998), pooling processing resources (Liederman 1998), and parallel processing (Compton 2002) among others. Bilaterally synchronous BOLD fluctuations have been previously observed in the motor cortex (Cordes et al. 2000), visual cortex, thalamus, and hippocampus of humans (Stein et al. 2000) and in the oculomotor and somatomotor areas of monkeys (Vincent et al. 2007). We report that the analogous brain areas of the rat also show bilaterally synchronous hemodynamic fluctuations. This suggests that interhemispheric synchronization of LFFs is phylogenetically preserved across all mammalian species and may underlie rudimentary brain functioning.

The observed bilateral synchrony of cortical and subcortical BOLD signals suggests inter-hemispheric neuronal connections. In the neocortex, the corpus callosum serves to interconnect most areas, while the smaller anterior commissure serves to connect the temporal neocortex. Studies of functional connectivity in patients with agenesis (Quigley et al. 2003) or resection (Johnston et al. 2008) of the corpus callosum have shown significantly decreased functional connectivity between the neocortices. It is therefore plausible that the observed bilateral synchrony of BOLD signals is a result of commissural connections between the two brain regions, but it remains to be confirmed for subcortical structures with weak commissural connections (e.g., caudate-putamen, hypothalamus).

Bilateral as well as unilateral components for the same functional area were observed in a number of rats from both anesthesia groups (Table 2). Using a model order of 40 components could have overestimated the number of networks in some rats, dividing the bilateral network of a functional area into two unilateral components. Previous human studies using ICA have also reported that functionally connected regions can split into separate components at high model order dimensionalities (Abou-Elseoud et al. 2010; Smith et al. 2009; van de Ven et al. 2004). It has been proposed that the stable components represent less connected nodes, while branching ones function as network connector hubs (Abou-Elseoud et al. 2010) though there is currently little quantitative evidence to support this.

The typical result in the present study was the presence of both bi- and unilateral components in the same animal. We believe that

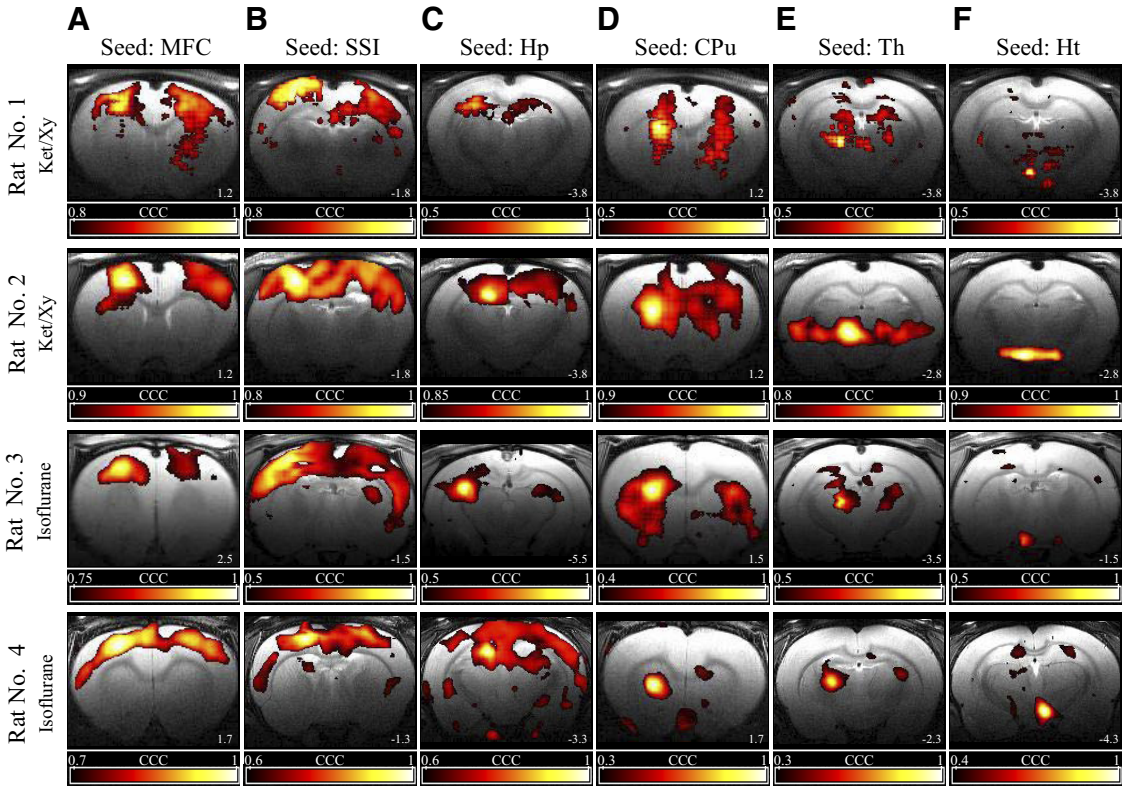

FIG. 3. Resting-state connectivity of representative ketamine/xylazine (Ket/Xy; *rats 1* and *2*) and isoflurane (*rats 3* and *4*) anesthetized rats derived using seed-region analysis. Cross-correlation coefficient (CCC) maps were calculated by correlating the time course of all voxels with the average time course of a spherical seed region (0.5 mm radius) in the medial frontal cortex (MFC; *A*), primary somatosensory cortex (SSI; *B*), hippocampus (Hp; *C*), caudate-putamen (CPu; *D*), thalamus (Th; *E*), or hypothalamus (Ht; *F*). Different CCC thresholds were used for each image, as indicated by the color bar below each image. Coronal images are displayed and distance (mm) from bregma is shown at the right lower corner of each image (positive anterior, negative posterior to bregma).

unilateral components represent the local connectivity, which is both independent and concurrent with the interhemispheric connectivity of each functional area. The ability of homologous brain areas to operate both uni- and bilaterally has been documented in behavioral and electrophysiological literature (Banich and Belger 1990; MacDonald et al. 1996; Nikouline et al. 2001). As an example, the left paw of the rat can operate independently of the right; however, both paws may also act in unison during a coordinated movement. Interestingly, Pawela and colleagues (2010) have shown significant disruption of sensorimotor interhemispheric LFFs following limb deafferentation while unilateral (intra-hemispheric) connectivity was preserved. Unilateral components may not be observed in animals with only a bilateral network component as a result of ICA underestimation or a high degree of temporal pattern similarity between local and interhemispheric networks. ICA would then be extracting a composite

TABLE 3. *Previously identified resting-state networks of the rat*

Reference	Anesthesia	Seed-Region Selection	Identified Networks	Other Findings
Kannurpatti et al. (2007)	Isoflurane (1.2%)	Stereotaxic atlas	Bilateral SI (sparse)	Blood extraction ↑ bilateral connectivity in cortex and Th
Zhao et al., 2007	Medetomidine (0.1 mg∗kg^{-1}∗h^{-1})	Paw stimulation	Bilateral SI bilateral CPu	Magnitude of LFFs similar to humans
Lu et al. (2007)	α-chloralose (30, 70, 100 mg∗kg^{-1}∗h^{-1})	Paw stimulation	Bilateral SI	↓ Bilateral connectivity with ↑ dose
Pawela et al. (2008)	Medetomidine (0.1 mg∗kg^{-1}∗h^{-1})	Nerve stimulation Light stimulation	Bilateral MI/MII, SI/SII, & Th bilateral VI/VII, SC, & Th	RPCC matrices show high correlations between many sensory/motor areas
Majeed et al. (2009)	α-chloralose (27 mg∗kg^{-1}∗h^{-1})	Paw stimulation	Bilateral SI/SII bilateral CPu	2 frequency peaks Dynamic LFFs
Pawela et al. (2010)	Medetomidine (0.1 mg∗kg^{-1}∗h^{-1})	Nerve stimulation Light stimulation	Bilateral MI/MII, SI/SII, & Th bilateral VI/VII, SC, & Th	Network changes following limb deafferentation

Individual thalamic nuclei have been grouped into the term thalamus as there is diffuse functional connectivity between these regions. CPu, caudate-putamen; LFFs, Low frequency fluctuations; MI, Primary motor cortex; MII, Secondary motor cortex; RPCC, Regional pair-wise correlation coefficient; SC, Superior colliculus; SI, Primary Somatosensory cortex; SII, Secondary somatosensory cortex; Th, Thalamus; VI, Primary visual cortex; VII, Secondary visual cortex.

of both underlying processes within the same network component (Seifritz et al. 2002).

Most networks for both groups were spatially symmetric as seen in Fig. 1. There are, however, networks in which the spatial extent of the clusters can be larger in one hemisphere (Fig. 1, lateral occipital cortex, isoflurane anesthesia). The "dominant" (increased ipsilateral cluster size) hemisphere varied within anesthesia groups and within the same rat for different networks (see supplementary figure).[1] This is commonly reported in seed-region investigations of humans, monkeys, and rats (Cordes et al. 2001; Lu et al. 2007; Vincent et al. 2007) in which placement of the seed predicts the larger cluster in that hemisphere. Previous investigations of resting-state networks using single-subject ICA have also extracted asymmetric functional networks (Fransson et al. 2009). This effect may not be as apparent in human studies using group ICA as individual hemispheric differences may be averaged out. Currently, the functional significance of this property is unknown but may reflect hemispheric dominance.

Anesthesia

The present study represents the first report of LFFs and resting-state network connectivity in the rat under ketamine/xylazine anesthesia. Ketamine, a noncompetitive *N*-methyl-D-aspartate (NMDA) receptor antagonist (Duncan et al. 1999) and xylazine, an α-2-adrenergic receptor agonist (Greene et al. 1998), are commonly used for animal anesthesia and have been increasingly used for imaging experiments (Hildebrandt et al. 2008; Wood et al. 2001). Use of this anesthetic regime in BOLD-fMRI has been limited to the study of nociceptive stimuli (Shih et al. 2008), electrically induced partial limbic seizures (Englot et al. 2009), and spinal cord investigations of the cat (Cohen-Adad et al. 2009). The present study confirms that the ketamine/xylazine combination is useful for the study of resting networks as substantial inter-hemispheric communication persisted over extended periods of time (e.g., during the 10-min scan). Its usefulness in task-elicited BOLD responses remains to be evaluated.

Isoflurane is a vasodilator (Farber et al. 1997) that can alter cerebrovascular activity and has been shown to have dose-dependent effects on task-elicited BOLD responses in the rat cortex (Masamoto et al. 2009). However, Vincent et al. (2007) reported that task-independent, coherent spontaneous BOLD fluctuations persisted in the monkey under increasing levels of isoflurane anesthesia though connectivity was decreased. A similar observation was also made in rats under α-chloralose (Lu et al. 2007). Using an isoflurane dose (1%) that approached the minimum required for maintaining immobility (Masamoto et al. 2009), the present study revealed more robust network activity than a previous report on isoflurane-anesthetized rats (Kannurpatti et al. 2008). However, there was no apparent difference in the resting-state LFFs under ketamine/xylazine and isoflurane anesthesia. Thus we extend the notion that resting-state LFFs persist under general anesthetics with different mechanisms of action, such as medetomidine (Pawela et al. 2008; Zhao et al. 2008), α-chloralose (Lu et al. 2007; Majeed et al. 2009), isoflurane (Kannurpatti et al. 2008), and now ketamine/xylazine. Taken together, we believe that resting hemodynamic fluctuations represent a ubiquitous intrinsic property of functional brain organization.

Physiological fluctuations

Physiological fluctuations due to respiration and cardiac movements can alias into the low-frequency range, which is used for connectivity mapping (Biswal et al. 1996; Fukunaga et al. 2006). Our BOLD signal sampling rate of 1 Hz could allow aliasing of the rat breathing (~1 Hz) and heart (4–6 Hz) rate. A higher sampling rate could prevent aliasing, but it would greatly reduce image resolution and the number of slices acquired. The result that ICA components were found in localized areas, or selectively in homologous areas of both hemispheres, cannot be attributed to physiological fluctuations. The temporal patterns and power spectra of the different network components were distinct and not indicative of a common source. In addition, signals that share a single source, such as respiration will be isolated following the ICA processing. As shown by De Luca and colleagues (2006) in human studies and argued by Zhao et al. (2008) for rats, a substantial contribution of autoregulation of the cerebral vasculature to the observed network connectivity is unlikely.

Conclusions

Using ICA of the BOLD signals, we inferred that the rat brain is composed of multiple, independent functional networks that involve cortical and subcortical structures. The functional connectivity among multiple structures was revealed in a single scanning session without the use of a motor task or a sensory stimulus. This will facilitate future studies of the mechanisms and function of the resting-state under physiological and pathological conditions.

ACKNOWLEDGMENTS

The authors thank M. Bellyou-Camilleri and A. Li for technical assistance.

GRANTS

Canadian Institutes of Health Research Grant 15685.

DISCLOSURES

No conflicts of interest are declared by the authors.

REFERENCES

Abou-Elseoud A, Starck T, Remes J, Nikkinen J, Tervonen O, Kiviniemi V. The effect of model order selection in group PICA. *Hum Brain Mapp* In press.

Banich MT, Belger A. Interhemispheric interaction: how do the hemispheres divide and conquer a task? *Cortex* 26: 77–94, 1990.

Banich MT. The missing link: the role of interhemispheric interaction in attentional processing. *Brain Cogn* 36: 128–157, 1998.

Beckmann CF, DeLuca M, Devlin JT, Smith SM. Investigations into resting-state connectivity using independent component analysis. *Philos Trans R Soc Lond B Biol Sci* 360: 1001–1013, 2005.

Bell AJ, Sejnowski TJ. An information-maximization approach to blind separation and blind deconvolution. *Neural Comput* 7: 1129–1159, 1995.

Biswal B, DeYoe EA, Hyde JS. Reduction of physiological fluctuations in fMRI using digital filters. *Magn Reson Med* 35:117–123, 1996.

Biswal B, Yetkin FZ, Haughton VM, Hyde JS. Functional connectivity in the motor cortex of resting human brain using echo-planar MRI. *Magn Reson Med* 34: 537–541, 1995.

[1] The online version of this article contains supplemental data.

Bluhm RL, Miller J, Lanius RA, Osuch EA, Boksman K, Neufeld RW, Théberge J, Schaefer B, Williamson P. Spontaneous low-frequency fluctuations in the BOLD signal in schizophrenic patients: anomalies in the default network. *Schizophr Bull* 33: 1004–1012, 2007.

Calhoun VD, Adali T, McGinty VB, Pekar JJ, Watson TD, Pearlson GD. fMRI activation in a visual-perception task: network of areas detected using the general linear model and independent components analysis. *Neuroimage* 14: 1080–1088, 2001.

Cherkassky VL, Kana RK, Keller TA, Just MA. Functional connectivity in a baseline resting-state network in autism. *Neuroreport* 17: 1687–1690, 2006.

Cohen-Adad J, Hoge RD, Leblond H, Xie G, Beaudoin G, Song AW, Krueger G, Doyon J, Benali H, Rossignol S. Investigations on spinal cord fMRI of cats under ketamine. *Neuroimage* 44: 328–339, 2009.

Cole DM, Smith SM, Beckmann CF. Advances and pitfalls in the analysis and interpretation of resting-state FMRI data. *Front Syst Neurosci* 4: 8, 2010.

Compton RJ. Inter-hemispheric interaction facilitates face processing. *Neuropsychologia* 40: 2409–2419, 2002.

Cordes D, Haughton VM, Arfanakis K, Carew JD, Turski PA, Moritz CH, Quigley MA, Meyerand ME. Frequencies contributing to functional connectivity in the cerebral cortex in "resting-state" data. *Am J Neuroradiol* 22: 1326–1333, 2001.

Cordes D, Haughton VM, Arfanakis K, Wendt GJ, Turski PA, Moritz CH, Quigley MA, Meyerand ME. Mapping functionally related regions of brain with functional connectivity MRI. *Am J Neuroradiol* 21: 1636–1644, 2000.

Correa N, Adali T, Calhoun VD. Performance of blind source separation algorithms for fMRI analysis using a group ICA method. *Magn Reson Imaging* 25: 684–694, 2007.

De Luca M, Beckmann CF, De Stefano N, Matthews PM, Smith SM. fMRI resting state networks define distinct modes of long-distance interactions in the human brain. *Neuroimage* 29: 1359–1367, 2006.

Duncan GE, Miyamoto S, Leipzig JN, Lieberman JA. Comparison of brain metabolic activity patterns induced by ketamine, MK-801 and amphetamine in rats: support for NMDA receptor involvement in responses to subanesthetic dose of ketamine. *Brain Res* 843: 171–183, 1999.

Englot DJ, Modi B, Mishra AM, DeSalvo M, Hyder F, Blumenfeld H. Cortical deactivation induced by subcortical network dysfunction in limbic seizures. *J Neurosci* 29: 13006–13018, 2009.

Farber NE, Harkin CP, Niedfeldt J, Hudetz AG, Kampine JP, Schmeling WT. Region-specific and agent-specific dilation of intracerebral microvessels by volatile anesthetics in rat brain slices. *Anesthesiology* 87: 1191–1198, 1997.

Fransson P, Skiöld B, EngströM M, Hallberg B, Mosskin M, Aden U, Lagercrantz H, Blennow M. Spontaneous brain activity in the newborn brain during natural sleep–an fMRI study in infants born at full term. *Pediatr Res* 66: 301–305, 2009.

Fukunaga M, Horovitz SG, van Gelderen P, de Zwart JA, Jansma JM, Ikonomidou VN, Chu R, Deckers RHR, Leopold DA, Duyn JH. Large-amplitude, spatially correlated fluctuations in BOLD fMRI signals during extended rest and early sleep stages. *Magn Reson Imaging* 24: 979–992, 2006.

Gerloff C, Andres FG. Bimanual coordination and interhemispheric interaction. *Acta Psychol* 110: 161–186, 2002.

GIFT. Group ICA of fMRI Toolbox (GIFT). http://icatb.sourceforge.net, 2008.

Greene SA, Thurmon JC. Xylazine–a review of its pharmacology and use in veterinary medicine. *J Vet Pharmacol Ther* 11: 295–313, 1998.

Greicius MD, Flores BH, Menon V, Glover GH, Solvason HB, Kenna H, Reiss AL, Schatzberg AF. Resting-state functional connectivity in major depression: abnormally increased contributions from subgenual cingulate cortex and thalamus. *Biol Psychiatry* 62: 429–437, 2007.

Greicius MD, Srivastava G, Reiss AL, Menon V. Default-mode network activity distinguishes Alzheimer's disease from healthy aging: evidence from functional MRI. *Proc Natl Acad Sci USA* 101: 4637–4642, 2004.

Greicius MD, Supekar K, Menon V, Dougherty RF. Resting-state functional connectivity reflects structural connectivity in the default mode network. *Cereb Cortex* 19: 72–78, 2009.

Hampson M, Peterson BS, Skudlarski P, Gatenby JC, Gore JC. Detection of functional connectivity using temporal correlations in MR images. *Hum Brain Mapp* 15: 247–262, 2002.

Hildebrandt IJ, Su H, Weber WA. Anesthesia and other considerations for in vivo imaging of small animals. *ILAR J* 49: 17–26, 2008.

Houzel JC, Carvalho ML, Lent R. Interhemispheric connections between primary visual areas: beyond the midline rule. *Braz J Med Biol Res* 35: 1441–1453, 2002.

Johnston JM, Vaishnavi SN, Smyth MD, Zhang D, He BJ, Zempel JM, Shimony JS, Snyder AZ, Raichle ME. Loss of resting interhemispheric functional connectivity after complete section of the corpus callosum. *J Neurosci* 28: 6453–6458, 2008.

Kannurpatti SS, Biswal BB, Kim YR, Rosen BR. Spatio-temporal characteristics of low-frequency BOLD signal fluctuations in isoflurane-anesthetized rat brain. *Neuroimage* 40: 1738–1747, 2008.

Klassen LM, Menon RS. Robust automated shimming technique using arbitrary mapping acquisition parameters (RASTAMAP). *Magn Reson Med* 51: 881–887, 2004.

Laufs H, Krakow K, Sterzer P, Eger E, Beyerle A, Salek-Haddadi A, Kleinschmidt A. Electroencephalographic signatures of attentional and cognitive default modes in spontaneous brain activity fluctuations at rest. *Proc Natl Acad Sci USA* 100: 11053–11058, 2003.

Liederman J. The dynamics of interhemispheric collaboration and hemispheric control. *Brain Cogn* 36: 193–208, 1998.

Lin W, Zhu Q, Gao W, Chen Y, Toh CH, Styner M, Gerig G, Smith JK, Biswal B, Gilmore JH. Functional connectivity MR imaging reveals cortical functional connectivity in the developing brain. *Am J Neuroradiol* 29: 1883–1889, 2008.

Lowe MJ, Phillips MD, Lurito JT, Mattson D, Dzemidzic M, Mathews VP. Multiple sclerosis: Low-frequency temporal blood oxygen level-dependent fluctuations indicate reduced functional connectivity initial results. *Radiology* 224: 184–192, 2002.

Lu H, Zuo Y, Gu H, Waltz JA, Zhan W, Scholl CA, Rea W, Yang Y, Stein EA. Synchronized delta oscillations correlate with the resting-state functional MRI signal. *Proc Natl Acad Sci USA* 104: 18265–18269, 2007.

MacDonald KD, Brett B, Barth DS. Inter- and intra-hemispheric spatiotemporal organization of spontaneous electrocortical oscillations. *J Neurophysiol* 76: 423–437, 1996.

Majeed W, Magnuson M, Keilholz SD. Spatiotemporal dynamics of low frequency fluctuations in BOLD fMRI of the rat. *J Magn Reson Imaging* 30: 384–393, 2009.

Mannell MV, Franco AR, Calhoun VD, Cañive JM, Thoma RJ, Mayer AR. Resting state and task-induced deactivation: a methodological comparison in patients with schizophrenia and healthy controls. *Hum Brain Mapp* 31: 424–437, 2010.

Masamoto K, Fukuda M, Vazquez A, Kim SG. Dose-dependent effect of isoflurane on neurovascular coupling in rat cerebral cortex. *Eur J Neurosci* 30: 242–250, 2009.

McKeown MJ, Makeig S, Brown GG, Jung TP, Kindermann SS, Bell AJ, Sejnowski TJ. Analysis of fMRI data by blind separation into independent spatial components. *Hum Brain Mapp* 6: 160–188, 1998.

Mirsattari SM, Bihari F, Leung LS, Menon RS, Wang Z, Ives JR, Bartha R. Physiological monitoring of small animals during magnetic resonance imaging. *J Neurosci Methods* 144: 207–213, 2005.

Morcom AM, Fletcher PC. Does the brain have a baseline? Why we should be resisting a rest. *Neuroimage* 37: 1073–1082, 2007.

Nikouline VV, Linkenkaer-Hansen K, Huttunen J, Ilmoniemi RJ. Interhemispheric phase synchrony and amplitude correlation of spontaneous beta oscillations in human subjects: a magnetoencephalographic study. *Neuroreport* 12: 2487–2491, 2001.

Pawela CP, Biswal BB, Cho YR, Kao DS, Li R, Jones SR, Schulte ML, Matloub HS, Hudetz AG, Hyde JS. Resting-state functional connectivity of the rat brain. *Magn Reson Med* 59: 1021–1029, 2008.

Pawela CP, Biswal BB, Hudetz AG, Li R, Jones SR, Cho YR, Matloub HS, Hyde JS. Interhemispheric neuroplasticity following limb deafferentation detected by resting-state functional connectivity magnetic resonance imaging (fcMRI) and functional magnetic resonance imaging (fMRI). *Neuroimage* 49: 2467–2478, 2010.

Paxinos G, Watson C. *The Rat Brain in Stereotaxic Coordinates.* New York: Academic, 1986.

Quigley M, Cordes D, Turski P, Moritz C, Haughton V, Seth R, Meyerand ME. Role of the corpus callosum in functional connectivity. *Am J Neuroradiol* 24: 208–212, 2003.

Raichle ME, MacLeod AM, Snyder AZ, Powers WJ, Gusnard DA, Shulman GL. A default mode of brain function. *Proc Natl Acad Sci USA* 98: 676–682, 2001.

Rest. Resting-State fMRI Data Analysis Toolkit (REST). Song, X, Yan, C, Dong, Z. (http://www.restfmri.net), 2007.

Seifritz E, Esposito F, Hennel F, Mustovic H, Neuhoff JG, Bilecen D, Tedeschi G, Scheffler K, Di Salle F. Spatiotemporal pattern of neural processing in the human auditory cortex. *Science* 297: 1706–1708, 2002.

Shih YY, Chang C, Chen JC, Jaw FS. BOLD fMRI mapping of brain responses to nociceptive stimuli in rats under ketamine anesthesia. *Med Eng Phys* 30: 953–958, 2008.

Smith SM, Fox PT, Miller KL, Glahn DC, Fox PM, Mackay CE, Filippini N, Watkins KE, Toro R, Laird AR, Beckmann CF. Correspondence of the brain's functional architecture during activation and rest. *Proc Natl Acad Sci USA* 106: 13040–13045, 2009.

Stein T, Moritz C, Quigley M, Cordes D, Haughton V, Meyerand M. Functional connectivity in the thalamus and hippocampus studied with fMRI. *Am J Neuroradiol* 21: 1397–1401, 2000.

van DE Ven VG, Formisano E, Prvulovic D, Roeder CH, Linden DE. Functional connectivity as revealed by spatial independent component analysis of fMRI measurements during rest. *Hum Brain Mapp* 22: 165–178, 2004.

Vanhatalo S, Palva JM, Holmes MD, Miller JW, Voipio J, Kaila K. Infraslow oscillations modulate excitability and interictal epileptic activity in the human cortex during sleep. *Proc Natl Acad Sci USA* 101: 5053–5057, 2004.

Vigário R, Särelä J, Jousmäki V, Hämäläinen M, Oja E. Independent component approach to the analysis of EEG and MEG recordings. *IEEE Trans Biomed Eng* 47: 589–593, 2000.

Vincent JL, Patel GH, Fox MD, Snyder AZ, Baker JT, Van Essen DC, Zempel JM, Snyder LH, Corbetta M, Raichle ME. Intrinsic functional architecture in the anaesthetized monkey brain. *Nature* 447: 83–86, 2007.

Vincent JL, Snyder AZ, Fox MD, Shannon BJ, Andrews JR, Raichle ME, Buckner RL. Coherent spontaneous activity identifies a hippocampal-parietal memory network. *J Neurophysiol* 96: 3517–3531, 2006.

Waites AB, Briellmann RS, Saling MM, Abbott DF, Jackson GD. Functional connectivity networks are disrupted in left temporal lobe epilepsy. *Ann Neurol* 59: 335–343, 2006.

Wood AK, Klide AM, Pickup S, Kundel HL. Prolonged general anesthesia in MR studies of rats. *Acad Radiol* 8: 1136–1140, 2001.

Zhao F, Zhao T, Zhou L, Wu Q, Hu X. BOLD study of stimulation-induced neural activity and resting-state connectivity in medetomidine-sedated rat. *Neuroimage* 39: 248–260, 2008.